Published in final edited form as:
Phys Med Biol. 2008 December 21; 53(24): 7107–7124. doi:10.1088/0031-9155/53/24/007.

Magnetization transfer proportion: a simplified measure of dose response for polymer gel dosimetry

Heather M Whitney[1,2], **Daniel F Gochberg**[1,2,3], and **John C Gore**[1,2,3,4]

1 *Vanderbilt University Institute of Imaging Science, Nashville, TN 37232-2675, USA*

2 *Department of Physics and Astronomy, Vanderbilt University, Nashville, TN 37232-2675, USA*

3 *Department of Radiology and Radiological Sciences, Vanderbilt University, Nashville, TN 37232-2675, USA*

4 *Department of Biomedical Engineering, Vanderbilt University, Nashville, TN 37232-2675, USA*

Abstract

The response to radiation of polymer gel dosimeters has most often been described by measuring the nuclear magnetic resonance transverse relaxation rate as a function of dose. This approach is highly dependent upon the choice of experimental parameters, such as the echo spacing time for Carr-Purcell-Meiboom-Gill-type pulse sequences, and is difficult to optimize in imaging applications where a range of doses are applied to a single gel, as is typical for practical uses of polymer gel dosimetry. Moreover, errors in computing dose can arise when there are substantial variations in the radiofrequency (B_1) field or resonant frequency, as may occur for large samples. Here we consider the advantages of using magnetization transfer imaging as an alternative approach and propose the use of a simplified quantity, the magnetization transfer proportion (MTP), to assess doses. This measure can be estimated through two simple acquisitions and is more robust in the presence of some sources of system imperfections. It also has a dependence upon experimental parameters that is independent of dose, allowing simultaneous optimization at all dose levels. The MTP is shown to be less susceptible to B_1 errors than are CPMG measurements of R_2. The dose response can be optimized through appropriate choices of the power and offset frequency of the pulses used in magnetization transfer imaging.

1. Introduction

Polymer gel dosimeters comprise an aqueous matrix in which various monomers are uniformly distributed. The monomers convert to polymers upon irradiation, so that various local properties are modified in a dose-dependent fashion. The resulting spatial pattern of dose deposition can be read out using one of several methods, including magnetic resonance imaging (MRI) (Maryanski *et al* 1993) and optical (Gore *et al* 1996) and X-ray computed tomography methods (Hilts *et al* 2000). Most practical applications to date have used MRI, and the dose response has usually been described in terms of the transverse relaxation rate, R_2 (Maryanski *et al* 1994). Alternative imaging metrics have also been investigated, including magnetization transfer (MT) imaging (Lepage *et al* 2002). MT imaging is sensitive to the exchange of magnetization between proton pools in a sample that results from chemical exchange or through-space dipolar interactions (Wolff and Balaban 1989, Henkelman *et al* 1993). In a simple model that may be appropriate for polymer gels, two distinct proton populations are considered to be coupled together. One pool corresponds to the mobile solvent protons, and a

E-mail: heather.whitney@vanderbilt.edu

second pool corresponds to hydrogen nuclei that are relatively immobile, associated with the polymer in some way, and have different relaxation times or different resonant frequencies because of chemical-shift effects. The integrated signal from both pools is measured after the application of an appropriate saturating RF pulse at a frequency that is off-resonance to the free water. The magnetization transfer ratio (MTR) has often been used as an index of the degree of MT. It is defined as

$$\mathrm{MTR}=\frac{M_0 - M_{\mathrm{sat}}}{M_0}, \tag{1}$$

where M_0 is the signal of the sample acquired without off-resonance saturation and M_{sat} is the signal acquired with saturation. Gel dosimetry measurements of MT have used slightly different assessments of the magnetization measured with and without saturation. For example, De Deene *et al* (2006b) proposed the 'true magnetization transfer ratio' which incorporates the direct effect of the saturating irradiation on the free water. This ratio is given by

$$\mathrm{MT}=\frac{M_{\mathrm{H_2O}} - M_{\mathrm{sat}}}{M_0}=\mathrm{MTR} - \frac{M_{\mathrm{dir}}}{M_0}, \tag{2}$$

where M_{H2O} is the experimentally measured magnetization of water after a saturation pulse has been applied and M_{dir} is described by the authors of the work to be the 'direct effect contribution which is due to the saturation of the water proton pool'. Other studies have published values for the specific parameters that contribute to MT for different types of polymer gel dosimeters as a function of dose (Gochberg *et al* 2001, 2003).

The aim of this paper is to provide a theoretical and experimental basis for using a slightly different ratio of MT measurements for gel dosimetry that results in a linear response of this quantity with dose in the range of 0–20 Gy. This approach will be compared to the more traditional transverse relaxation rate measurement for dosimetry gels. In particular, the relative sensitivities of the MT and transverse relaxation dose responses to the effects of imperfections in imaging, including errors in the amplitudes of the radiofrequency pulses used, are evaluated.

2. Theory

2.1. Dose response

Traditional transverse relaxation rate measurements of polymer gel dosimeters are performed using spin–echo imaging. Assuming that the system is not saturated (i.e. TR $\gg$ T_1), the signal at echo time TE is given by

$$S=M_0\, \mathrm{e}^{-R_2\mathrm{TE}}. \tag{3}$$

In a region of linear dose response,

$$R_2=R_{2,0}+\alpha D, \tag{4}$$

where α and $R_{2,0}$ are the slope and intercept, respectively. The signal difference generated by any small dose increment ΔD is then

$$\Delta S = -\alpha \cdot \mathrm{TE} \cdot S \cdot \Delta D. \tag{5}$$

This has a maximum value when TE = $1/R_2$, when the signal change is

$$\Delta S = -0.37\frac{\alpha}{R_{2,0}+\alpha D}\Delta D \cdot M_0, \tag{6}$$

and decreases with dose D. For the most sensitive PAG and MAGIC gels, α is 0.19 and 0.503, and $R_{2,0}$ is 0.9 and 7.653, respectively (De Deene *et al* 2006a, Luci *et al* 2007). Thus, compared to the signal of an unirradiated dosimeter, a dose of 1 Gy will decrease the gel MRI signal by $0.064M_0$ and $0.151M_0$ initially for PAG and MAGIC gels, respectively, but this decreases to only $0.011M_0$ and $0.015M_0$, respectively, when comparing doses at 20 Gy, even at the optimal echo spacing for that dose. The situation is further compromised because R_2 may vary throughout the gel so no single choice of TE is then optimal for all regions. Thus, even without considering errors inherent in calculating values of R_2 from multiple echo data, the signal changes available for discriminating regions of similar doses are small. A further complication occurs in multi-echo sequences, which can produce maps of R_2 from a single acquisition but are sensitive to RF and static field inhomogeneities (Majumdar *et al* 1986a, 1986b), and the precise value of T_2 may depend on the echo spacing (Baldock *et al* 2001).

A simple method using only two images, and from which a quantity that varies approximately linearly with dose can be easily extracted, would be attractive. A simple MT-sensitive imaging sequence is one that incorporates an off-resonance saturating pulse immediately prior to imaging. The off-resonance pulse can be designed to saturate the immobile or chemically shifted protons and to not affect the free water resonance directly. MT effects alone then cause the signal from the mobile protons to decrease. This approach is the conventional MT imaging option available on commercial MRI systems.

The effect of the off-resonance saturating irradiation is to reduce the signal of the mobile water from M_0 to M_{sat}. The residual MRI signal is given by (Henkelman *et al* 1993)

$$\frac{M_{\text{sat}}}{M_0} = \frac{R_{1,m}k_{fm}+R_{1,f}R_{rf,m}+R_{1,f}R_{1,m}+R_{1,f}k_{mf}}{\left(R_{1,f}+R_{rf,f}+k_{fm}\right)\left(R_{1,m}+R_{rf,m}+k_{mf}\right)-k_{mf}k_{fm}}. \tag{7}$$

In this model, suppose the subscript '*f*' stands for the free water pool and '*m*' for a second proton pool which has more efficient relaxation and a broader resonance or is chemically shifted. This pool represents the polymerized product of irradiation and increases in direct proportion to the degree of polymerization and dose, a linear approximation to an exponential change (Lepage *et al* 2001). R_1 is the longitudinal magnetization rate constant, k_{mf} and k_{fm} are the rates of MT from the polymer pool to the free pool and vice versa, respectively, and $R_{rf,i}$ is the rate of loss of longitudinal magnetization in either the free or other pool. If we take $R_{rf,f}$ to be zero and $R_{rf,m}$ to be much greater than all other rates, as is the case in an ideal MT experiment, equation (7) becomes

$$\frac{M_{\text{sat}}}{M_0} = \frac{R_{1,f}}{R_{1,f}+k_{fm}}. \tag{8}$$

For the rest of the discussion, $R_{1,f}$ and k_{fm} will be referred to as R_1 and k, respectively, to simplify notation. M_{sat} and M_0 can be rearranged to give

$$\frac{M_0 - M_{\text{sat}}}{M_{\text{sat}}} = \frac{k}{R_1}. \tag{9}$$

We will call the ratio $\frac{M_0 - M_{\text{sat}}}{M_{\text{sat}}}$ the magnetization transfer proportion (MTP). The MTR is related to the MTP:

$$\text{MTR} = \frac{M_0 - M_{\text{sat}}}{M_0} = \frac{k}{R_1 + k}; \quad \text{MTP} = \frac{\text{MTR}}{1 - \text{MTR}}. \tag{10}$$

The rate constant k will increase with dose in proportion to the amount of polymer produced, as has been shown to be the case for methacrylic-based dosimeter gels in the dose range of 0–20 Gy (Gochberg *et al* 2003). We therefore may write

$$k = k_0 + \beta D. \tag{11}$$

We then have

$$\text{MTP} = k_0 T_1 + \beta T_1 D. \tag{12}$$

To calculate the MTP, two images (M_0, M_{sat}) must be measured, which then can be combined to produce a quantity that should vary linearly with dose. The slope of this dose response is

$$\beta T_1 = \frac{\beta}{R_1}. \tag{13}$$

The ratio of the slope to the intercept of the dose response is a useful indicator of sensitivity when considering the detectibility of small changes in dose (Fong *et al* 2001); for the MT measure this is $\frac{\beta}{k_0}$, compared with $\frac{\alpha}{R_{2,0}}$ for methods measuring transverse relaxation.

Equation (9) may also be derived by considering the relationship of M_{sat} to M_0 as given by (Wolff and Balaban 1989)

$$M_{\text{sat}} = M_0 (1 - k T_{1\,\text{sat}}), \tag{14}$$

where $T_{1\text{sat}}$ is the spin lattice relaxation time of the mobile water in the presence of the RF irradiation and is given by

$$\frac{1}{T_{1\,\text{sat}}} = \frac{1}{T_1} + k. \tag{15}$$

A manipulation of the quantities M_{sat} and M_0 results in the same relationship found in equation (9).

Equations (9) and (10) illustrate an advantage in calculating the effect of MT in terms of the MTP: if k is linear in dose (as given in equation (11)), so is MTP, but not MTR, even though fundamentally it contains the same information.

The interpretation of the MT–dose relationship can be further understood by considering a two-pool model of MT in more detail, such as that suggested by the results of measurements by Gochberg *et al* (2003). We can then write the second population as

$$p_m = p_m^0 + \gamma D, \tag{16}$$

where p_m is the size of the relevant polymer proton pool after irradiation, p_m^0 is the size of this second pool in the unirradiated dosimeter, D is the absorbed dose and γ is the slope of the pool size versus dose relationship. The MT rate constant, in the nomenclature introduced by Gochberg *et al* (2003), is then

$$k = k_{mf}\frac{p_m}{p_f} = k_{mf}\frac{p_m^0 + \gamma D}{p_f}, \tag{17}$$

ignoring the (insignificant) changes in p_f. Thus the slope of MTP versus D, as given in equation (9) and incorporating equation (17), is $\frac{k_{mf}\gamma}{p_f R_1}$. We may also note that for a two-pool exchange model of transverse relaxation

$$R_2 = R_{2f} + k_{mf}\frac{p_m}{p_f}. \tag{18}$$

Thus for this model, α, the slope of the R_2 versus dose line, is $\frac{k_{mf}\gamma}{p_f}$; thus the ratio $\frac{\alpha}{R_{2,0}} = \frac{k_{mf}\gamma}{p_f R_{2,0}}$. We see that mapping R_2 and the MTP are fundamentally related, both reflecting increases in the contribution of the fraction of polymer gel. However, the fractional increase in R_2 per dose is smaller than the increase in MTP by the ratio $\frac{R_2}{R_1}$, which can be as large as 10. Moreover, the slope-to-intercept ratio for the MT-based approach is $\frac{\gamma}{p_m^0}$ whereas for the conventional R_2 method it is $\frac{\gamma}{p_m^0 + \frac{p_f R_{2f}}{k_{mf}}}$, which is clearly smaller.

2.2. Effects of B_1 inhomogeneities

Both quantitative R_2 imaging and MTP imaging are vulnerable to variations and inaccuracies in the RF (B_1) field. Significant variations of the B_1 amplitude occur within large samples, especially at higher fields, so the flip angle experienced by any part of the sample may be in error from the ideal intended value. The sensitivity of multi-echo measurements of R_2 to such errors has been well documented (Majumdar *et al* 1986b, Sled and Pike 2000a). When the refocusing pulses in a CPMG sequence are not precisely 180°, the percent deviation in estimating T_2 is a function of T_2 itself; i.e. samples with higher T_2 value (and lower R_2) experience higher fractional deviations in T_2 (and thus, dose extracted from a calibration curve) for a given error in B_1 than samples of lower T_2. These inaccuracies in transverse relaxation

time estimates can result in an apparent nonlinearity of R_2 versus dose and miscalibration of the dose response curve.

The susceptibility of MT measurements to variations in B_1 has not been as thoroughly explored. In practice, the RF pre-pulse may produce incomplete saturation of the broad component and/or partial saturation of the narrow water resonance. An apparent linear dependence of the MTR on variations in B_1 has previously been reported (Samson *et al* 2006). We therefore have evaluated the effects of B_1 errors on estimates of dose in polymer gels for both the MTP and R_2 approaches.

3. Methods

3.1. Gel preparation and irradiation

MAGIC (9% methacrylic acid) and MAGIC-2 gel dosimeters were produced as previously described (Fong *et al* 2001, Luci *et al* 2007). The components of the two formulations are the same but in different proportions, as the MAGIC-2 formulation has been optimized for measurement of the transverse relaxation rate in the 0–20 Gy dose range. The manufacturing process was as follows: a Pyrex beaker containing the water for the desired volume of gel was placed in a water bath, along with a magnetic stirrer, on a hot plate. The desired quantity of gelatin was added and allowed to bloom. The temperature of the system was brought to 45 °C, at which point the water–gelatin solution was in liquid form. The monomer, ascorbic acid and cupric sulfate were added and the system was stirred for approximately 3 min. The solution was poured into 14 mL Pyrex screw-top test tubes and placed in a refrigerator until irradiation. Samples were brought to room temperature, immersed in a water bath and irradiated with 6 MV photons with a dose rate of 2.84 Gy min^{-1}. Total dose increments of 2 Gy were applied in a parallel-opposed fashion in sub-increments of 1 Gy each, in a range of 0–20 Gy. A single gel dosimeter from each formulation was removed after each application of 2 Gy of irradiation to create the set of gels in the desired range and dose separation. Samples were returned to refrigeration after irradiation. The MAGIC gels were manufactured 48 h before irradiation, and the MAGIC-2 gels were manufactured 24 h before irradiation.

3.2. Imaging measurements

After a refrigeration period of 9 days following irradiation, samples were allowed to come to room temperature and imaged at 4.7 T using a 31 cm bore Varian Inova (Varian Inc., Palo Alto, CA, USA) spectrometer using a 63 mm quadrature coil. The imaging matrix was 64 × 64, the field of view was 70 × 70 mm and the slice thickness was 4 mm. All samples from a given formulation were imaged together. MT imaging was performed with a MT-prepared spoiled gradient echo sequence (Sled and Pike 2000b), as this method is relatively fast and does not have the potential disadvantage of heating of the samples. To prevent stimulated echoes, spoiler gradients and rf spoiling were used to disperse transverse magnetization, and complete spoiling was assumed. A 10 ms Gaussian MT pulse was applied at 30 offset frequencies logarithmically distributed between 100 and 200 000 Hz for three different nominal MT pulse angles (283°, 566° and 849°), as well as at power levels of ±5 and 10% from each of these three powers. These powers are equivalent to 4.44, 8.88 and 13.32 μT, respectively (Tozer *et al* 2003, Tofts *et al* 2005). These powers were chosen to be representative of the strength of MT pulses available on clinical scanners. The signal was acquired via a 7° excitation sinc pulse. The TR was 25 ms and TE was 4 ms, and the data from two acquisitions were averaged together for each measurement.

Transverse relaxation measurements were made with a 32 echo CPMG-type pulse sequence with TR of 15 s and TE of 10 ms. The transverse relaxation time was estimated using a pixel-by-pixel fit (using Matlab's ‘robustfit’ function) of the log of the data to a linear model (see

equation (3)). Transverse relaxation rate maps were measured as a negative slope of the linear fit to the data for each pixel. One acquisition was taken for each measurement.

Reported values for MTP and R_2 were taken as the average value of pixels from a circular region (radius of 3 pixels) of interest for each sample.

4. Results

4.1. Magnetization transfer proportion measurements

Figure 1 displays an example MTP image of the data acquired from the MT experiment for the MAGIC-2 dosimeter. The image was created by applying equation (10) to images acquired for power of 8.88 μT at 200 000 Hz off-resonance (M_{sat}) and 1375 Hz off-resonance (M_0).

Figures 2 and 3 plot the measurement of the MTP for both types of MAGIC gel over a range of dose values, at four different offset frequencies and different MT powers. Each data point is the mean of a region of interest for each dosimeter, and the standard deviation is the standard deviation of those pixels in the region of interest.

There are a few important features to note from figures 2 and 3. Sensitivity, defined as the slope of the MTP versus dose, varies with the offset frequency and power of the MT pulse. At low powers and larger offsets the polymer pool is not fully saturated so the effects of MT are reduced. Additionally, there is a strong dependence of the intercept on the offset frequency and power chosen due to the direct effect of saturation on water, since it increases at small offsets, where the direct effect is strongest. This issue is addressed more fully in section 5. Given this lack of full saturation of the immobilized pool, we do not expect equation (9) or equation (14) to be valid at all offsets and powers. Indeed, in section 5, we consider how the theoretical expression for MTP should be modified under these circumstances. Nonetheless, our experimental data do in fact show linear responses, though with a slope and offset that depends upon the offset and power (in disagreement with equation (12), but as predicted below). In order to maximize dose sensitivity for MT measurements, the appropriate offset frequency and MT power should be chosen, as will be elaborated in section 5.

Tables 1 and 2 show values of the linear correlation coefficients R^2, a measure of how well these data are represented by a linear relationship, as a function of both offset frequency and power of the B_1 pulse, for the least-squares fit of MTP versus dose for MAGIC and MAGIC-2 dosimeters.

The slope and intercept of the dose response relationships can be combined to provide an assessment of dose response sensitivity (Fong *et al* 2001). Experimental values for these parameters for MTP are reported below. To aid in assessment of the performance of the MTP in the face of B_1 errors, the results acquired with the known B_1 error are also reported.

Tables 3 and 4 display the slope and intercept values calculated from a linear fit of the data acquired at different powers and a range of ±10% from the nominal powers, for the MAGIC-2 dosimeter. Values for the MAGIC dosimeter vary similarly.

Tables 5 and 6 display the calculated change in the slope-to-intercept ratio for the measured MTP of the MAGIC and MAGIC-2 dosimeter. With the exception of the MTP acquired for the MAGIC-2 dosimeter at the lowest power, the slope-to-intercept ratio of the MTP has a range of approximately ±15% for a range of −10 to +10% error in B_1 power.

4.2. Transverse relaxation simulation and measurement

The effect of B_1 errors on measurements of transverse relaxation has been well characterized in the literature. The observed value of R_2 due to a given error in B_1 power can be related as (Sled and Pike 2000a)

$$R_{2,\text{obs}}=R_2-\frac{\ln f}{\tau}, \tag{19}$$

where f is an attenuation factor and τ is the echo spacing of the CPMG-type experiment. The attenuation factor f incorporates the effect of errors due to imperfect B_1 pulses, and for a hard pulse sequence, assuming no error in B_0, is given by

$$f=\frac{\cos(\delta)}{2}-\cos(\delta)+\frac{1}{2}, \tag{20}$$

where δ is the degree of the refocusing B_1 pulse. Note that this derivation assumes that complete spoiling occurs of any transverse magnetization produced by incomplete nutations and stimulated echoes. Using experimental values for R_2 for the MAGIC and MAGIC-2 gel dosimeters and the above relationship, the expected deviation in R_2 due to a given error in B_1 can be calculated and the effect on the dose response can be estimated. The values used for the dosimeter from the experiment described above were 5.00 and 14.40 s^{-1} for the MAGIC dosimeter at 0 and 20 Gy, respectively, and 6.29 and 17.69 s^{-1} for the MAGIC-2 dosimeter. These values were calculated from a linear fit of the R_2 data acquired in the above experiment to simulate the kind of values that would be taken from a calibration curve. Figure 4 displays the expected variation in $R_{2,\text{obs}}$ for a given error in B_1 power for the MAGIC dosimeter as measured via a CPMG-type experiment using hard pulses.

The simulation shows that while the slope of the R_2 versus dose line remains the same (as indicated by the B_1-independent difference in R_2 between 20 and 0 Gy), the intercept (the value of R_2 at 0 Gy) will change significantly over a range of errors in B_1. Table 7 lists the expected percent change in the slope, intercept and slope–intercept ratio of R_2 versus dose for hypothetical errors in B_1 power.

4.3. Comparison of the effect of B_1 errors on dose estimates

Finally, a useful measure of the effect an error in B_1 power has on a measurement is to consider the apparent dose that would be calculated in the event of a specific B_1 variation. When polymer gel dosimeters are used for radiation field assessment, a calibration curve is created from dosimeters to which known doses are applied. The form of this line is

$$X=aD+b, \tag{21}$$

where X is the measured value, such as R_2 or MTP; a is the slope of the line and b is the intercept. Once the desired measurement is made of the dosimeter to be assessed for dose, the following equation is used to back-calculate to the apparent dose D_{app}:

$$D_{\text{app}}=\frac{X-b}{a}. \tag{22}$$

If the parameter, be it MTP or R_2, has been mis-measured due to B_1 errors, the apparent dose will be different than its true dose. This effect was investigated for the MTP and R_2 measurements in the MAGIC and MAGIC-2 dosimeters. The slope and intercept of the calibration curves for MTP data acquired with no B_1 error (the nominal B_1 powers referenced above) were applied to MTP values measured with a manually adjusted power with known error (±5 and 10% of the nominal B_1 power) using equation (22). Additionally, the slope and intercept calculated for the R_2 values were applied to simulated R_2 values acquired with a 5 and 10% B_1 error. The percent error in apparent dose was calculated as

$$\frac{D_{\text{app}} - D}{D} \times 100. \tag{23}$$

Figure 5 displays representative data of the percent error in apparent dose acquired in both MTP and R_2 measurements, as a function of applied dose. The data show that at lower dose levels, on the order of that which most radiation therapy dose fractionations deliver, measurements of MTP with a 10% error in B_1 show much less error in apparent dose than measurements of R_2.

5. Discussion

5.1. Saturation of the two pools

MT measurements of the dose response of gel dosimeters are potentially less dependent upon errors in B_1 power than traditional multi-echo measurements of the transverse relaxation rate. In principle, once sufficient B_1 power is applied off-resonance, complete saturation of the broad resonance can be achieved, and using larger powers will have little effect as long as direct saturation of the narrow water line is avoided.

At the powers and offsets shown in this work, complete saturation of the bound pool was not achieved, which may be more typical of conditions when using clinical scanners. The effect of incomplete saturation of the bound pool in the experiment can be estimated by adding a correction factor to equations (8) and (9), which were derived by taking $R_{rf,m}$ to be much greater than k, k_{mf}, R_1 and $R_{1,m}$. A first-order correction for incomplete macromolecular saturation can be derived by instead assuming that $R_{rf,m}$ and k_{mf} are much greater than k, R_1 and $R_{1,m}$. This gives

$$\frac{M_{\text{sat}}}{M_0} = \frac{R_1}{R_1 + k\left(1 - \frac{k_{mf}}{R_{rf,b} + k_{mf}}\right)}. \tag{24}$$

The quantity $1 - \frac{k_{mf}}{R_{rf,b} + k_{mf}}$ can be interpreted as a measure of the effect incomplete saturation has on measurements of MT. For the MTP, the inclusion of this error results in

$$\text{MTP} = \frac{k}{R_1}\left(1 - \frac{k_{mf}}{R_{rf,b} + k_{mf}}\right). \tag{25}$$

Equation (25) is strictly linear in dose only if k_{mf} is independent of dose, which is true for BANG gels (Gochberg *et al* 2001) but not MAGIC gels (Gochberg *et al* 2003). Hence, achieving complete saturation of the macromolecular pool would be ideal. Using published values for R_1, k and k_{mf} for the MAGIC gel dosimeter, the level of saturation (M_{sat}/M_0) achieved

in our experiments can be estimated via equation (24). These estimated values for dosimeters irradiated to 0 Gy are on the order of 84%, 65% and 53% saturation for the three powers (4.44, 8.88 and 13.32 μT, respectively) of the MT pulse in the experiment, while values for 20 Gy dosimeters are on the order of 76%, 49% and 33% for the three powers. The experiment was designed to perform the MT experiment at power levels similar to those available on clinical scanners, but the significant dependence of M_{sat}/M_0 on the rf power is due to incomplete saturation of the macromolecular pool.

It would be ideal to use known values for R_1, k and k_{mf} to estimate the appropriate MT power strength and offset frequency to use in MTP experiments. Such prior knowledge could aid in ensuring that the assumptions behind equations (9) and (11) are fully met. For example, prior work (Gochberg *et al* 2003) has estimated that for the MAGIC gel dosimeter, R_1, k and k_{mf} for dosimeters at 20 Gy are approximately 1 Hz, 7.2 Hz and 122 Hz, respectively. To estimate the range of powers and offsets for which $R_{rf,f}$ is much less than and $R_{rf,m}$ is much greater than any other rate, these values can be calculated using lineshape assumptions for the system in question and compared for the regime in which equations (9) and (11) are valid. Figure 6 displays calculations of the saturation of the free and bound pools and an assessment for whether or not the assumptions behind equations (9) and (11) were met. Values for $R_{rf,f}$ were calculated by assuming a Lorentzian lineshape for the free pool and using the relationship

$$R_{rf,f}=\frac{\omega_1^2 T_{2,f}}{1+\left(2\pi\Delta T_{2,f}\right)^2}, \tag{26}$$

where $T_{2,f}$ is the transverse relaxation time of the water pool, Δ is the offset frequency of the saturation and ω_1 is the strength of the MT pulse in rad s^{-1}. Values for $R_{rf,m}$ were calculated by assuming that the bound pool could be characterized by a Gaussian lineshape and using the relationship

$$R_{rf,m}=\omega_1^2 T_{2,m}\sqrt{\frac{\pi}{2}}T_{2,m}\,\mathrm{e}^{-\frac{\left(2\pi\Delta T_{2,m}\right)^2}{2}}, \tag{27}$$

where $T_{2,m}$ is the transverse relaxation time of the bound pool. For this value, an estimated value of 10 μs was used.

In figure 6(a), $R_{rf,f}$ is displayed as a function of both MT pulse power and frequency. Values greater than 1, approximately R_1 (the lowest rate of concern), are not plotted to preserve the scale of interest. Figure 6(b) displays $R_{rf,m}$. Figure 6(c) is displayed by evaluating at each offset frequency and MT power whether or not the criteria of $R_{rf,f} \ll$ all other rates and $R_{rf,m} \gg$ all other rates are valid, and the shaded area indicates the values for which the criteria are met.

A similar analysis can be used to appreciate the direct effect on the free water line. Assuming steady state conditions, the solution for the uncoupled Bloch equations for the transverse magnetization of the water is given by

$$\frac{M_{sat}}{M_0}=\frac{1+\left(\Delta T_{2,f}\right)^2}{1+\left(\Delta T_{2,f}\right)^2+\left(\frac{\omega_1}{2\pi}\right)^2 T_{1,f}T_{2,f}}. \tag{28}$$

Using values of $T_{2,f}$ of 1/14.4 Hz and assuming that R_1 is on the order of 1 Hz for polymer gel dosimeters at 4.7 T, the direct effect on the free water line can be estimated. Results for a range of frequency offsets and MT powers are displayed in figure 7.

It can be estimated from figure 7 that at the offset frequencies and powers in this work, there was some level of direct effect on the water (M_{sat}/M_0 having a range of approximately 40–70%), and this is likely another reason why our measurements of the MTP dose response intercept vary at the different offset frequencies.

These simulations suggest that while an appropriate range of offset frequencies was used for the measurement of MTP as displayed in figures 2 and 3, the MT power strength was less than ideal for a dosimeter with these specific relaxation properties. However, our results show that for clinically feasible implementation of MT experiments, where the power of the MT pulse may not be able to be increased by much or the user may only be able to set a nominal maximum power level, a linear dose response can still be attained. These results suggest that complete saturation of the macromolecular pool and *a priori* knowledge of the sample parameters are not necessary to achieve linearity in dose.

5.2. Comparison of dose measurement in the presence of B_1 errors

The change in the slope-to-intercept ratio for the measurement of the MTP in MAGIC-type gel dosimeters was approximately ±15%, while the value of the slope-to-intercept ratio for R_2 could be expected to deviate by as much as 33% for 10% error in B_1 power.

The estimated (apparent) dose at dose levels used in most fractionation schemes varies with B_1, but for the range of changes considered here the MTP appears less susceptible to errors in apparent dose than are measurements of R_2.

While the measurement of the MTP is linear in dose for a wide range of MT pulse powers and offset frequencies, it is important to note that the sensitivity can be maximized by the appropriate choice of these two variables. *A priori* knowledge of the MT rates for a particular type of dosimeter can be used to estimate the appropriate values for MT power and offset frequency, but as has been shown is not necessary to achieve a linear dose response of MTP.

The MTP approach has not been tested in polyacrylamide-type (PAG) polymer gel dosimeters. Some studies (Gochberg *et al* 2001, 2003) have suggested that MT may behave differently in PAG versus methacrylic acid-based dosimeters, which may affect the measurement of the MTP versus dose in PAG. Note also that the MTP is proportional to k (equation (9)) and inversely proportional to p_f, the size of the free pool (equation (17)), so efforts to change these may result in greater sensitivity. Sensitivity should also differ between dosimeters with different amounts of MT present due to formulation, as k_{mf} is dependent upon the amount of monomer. We have assumed, based on expectations and some experimental data, that k_{mf} is not dose dependent. In some conditions, this may no longer be valid (Gochberg *et al* 2003), such that $k_{mf} = k_{mf,0} +$ mD. Then, the MTP has both a linear and a quadratic term in terms of D. However, it will still appear linear until mD $\geq k_{mf,0}$.

The MTP has been described before in the imaging literature, using the name ‘equivalent cross-relaxation rate (ECR)’ (Sogami *et al* 2001), for imaging studies for breast cancer. However, the term ‘cross-relaxation’ has usually been reserved in nuclear magnetic resonance to denote dipolar cross-relaxation, whereas MT includes chemical exchange and other effects. We therefore feel it is not appropriate to use the ECR name and propose MTP for this quantity.

5.3. Other concerns

Image resolution should not significantly affect these types of measurements unless regions of interest are drawn such that partial volume effects are present in the measurement of the MTP. Creating regions of interest that are well within the boundaries of the samples will ensure that this error is avoided.

6. Conclusion

This work has shown that the measurement of the MTP in methacrylic acid-type gel dosimeters is linear with dose and shows promise as a measure of dose response in polymer gel dosimeters. The method has been validated at powers and offset frequencies similar to those used in clinical applications, and prior knowledge of magnetization transfer quantities, while desirable to maximize contrast, is not necessary to acquire useful dose response data. The method is less susceptible to calibration errors than transverse relaxation rate measurements in the presence of B_1 inhomogeneities.

Acknowledgments

The authors thank George Ding and Charles Coffey for assistance with dosimeter irradiation and Xiawei Ou for assistance with data acquisition. This work was supported by NIH grants CA090844, EB000214 and EB001452.

References

Baldock C, Lepage M, Back SAJ, Murry PJ, Jayasekera PM, Porter D, Kron T. Dose resolution in radiotherapy polymer gel dosimetry: effect of echo spacing in MRI pulse sequence. Phys. Med. Biol 2001;46:449–60. [PubMed: 11229725]

De Deene Y, Vergote K, Claeys C, De Wagter C. The fundamental radiation properties of normoxic polymer gel dosimeters: a comparison between a methacrylic acid based gel and acrylamide based gels. Phys. Med. Biol 2006a;51:653–73. [PubMed: 16424587]

De Deene Y, Vergote K, Claeys C, De Wagter C. Three dimensional radiation dosimetry in lung-equivalent regions by use of a radiation sensitive gel foam: proof of principle. Med. Phys 2006b; 33:2586–97. [PubMed: 16898463]

Fong PM, Keil DC, Does MD, Gore JC. Polymer gels for magnetic resonance imaging of radiation dose distributions at normal room atmosphere. Phys. Med. Biol 2001;46:3105–13. [PubMed: 11768494]

Gochberg DF, Fong PM, Gore JC. Studies of magnetization transfer and relaxation in irradiated polymer gels—interpretation of MRI-based dosimetry. Phys. Med. Biol 2001;46:799–811. [PubMed: 11277226]

Gochberg DF, Fong PM, Gore JC. A quantitative study of magnetization transfer in MAGIC gels. Phys. Med. Biol 2003;48:N277–82. [PubMed: 14653567]

Gore JC, Ranade M, Maryanski MJ, Schulz RJ. Radiation dose distributions in three dimensions from tomographic optical density scanning of polymer gels: 1. Development of an optical scanner. Phys. Med. Biol 1996;41:2695–704. [PubMed: 8971963]

Henkelman RM, Huang XM, Xiang QS, Stanisz GJ, Swanson SD, Bronskill MJ. Quantitative interpretation of magnetization-transfer. Magn. Reson. Med 1993;29:759–66. [PubMed: 8350718]

Hilts M, Audet C, Duzenli C, Jirasek A. Polymer gel dosimetry using x-ray computed tomography: a feasibility study. Phys. Med. Biol 2000;45:2559–71. [PubMed: 11008956]

Lepage M, Mcmahon K, Galloway GJ, De Deene Y, Back SAJ, Baldock C. Magnetization transfer imaging for polymer gel dosimetry. Phys. Med. Biol 2002;47:1881–90. [PubMed: 12108773]

Lepage M, Whittaker AK, Rintoul L, Baldock C. C-13-NMR, H-1-NMR, and FT-Raman study of radiation-induced modifications in radiation dosimetry polymer gels. J. Appl. Polym. Sci 2001;79:1572–81.

Luci JJ, Whitney HM, Gore JC. Optimization of MAGIC gel formulation for three-dimensional radiation therapy dosimetry. Phys. Med. Biol 2007;52:N241. [PubMed: 17473340]

Majumdar S, Orphanoudakis SC, Gmitro A, Odonnell M, Gore JC. Errors in the measurements of T2 using multiple-echo MRI techniques: 1. Effects of radiofrequency pulse imperfections. Magn. Reson. Med 1986a;3:397–417. [PubMed: 3724419]

Majumdar S, Orphanoudakis SC, Gmitro A, Odonnell M, Gore JC. Errors in the measurements of T2 using multiple-echo MRI techniques: 2. Effects of static-field inhomogeneity. Magn. Reson. Med 1986b;3:562–74. [PubMed: 3747818]

Maryanski MJ, Gore JC, Kennan RP, Schulz RJ. NMR relaxation enhancement in gels polymerized and cross-linked by ionizing radiation: a new approach to 3D dosimetry by MRI. Magn. Reson. Imaging 1993;11:253–8. [PubMed: 8455435]

Maryanski MJ, Schulz RJ, Ibbott G, Gatenby JC, Xie J, Horton D, Gore JC. Magnetic resonance imaging of radiation dose distributions using a polymer-gel dosimeter. Phys. Med. Biol 1994;39:1437–55. [PubMed: 15552115]

Samson RS, Wheeler-Kingshott CAM, Symms MR, Tozer DJ, Tofts PS. A simple correction for B-1 field errors in magnetization transfer ratio measurements. Magn. Reson. Imaging 2006;24:255–63. [PubMed: 16563954]

Sled JG, Pike GB. Correction for B-1 and B-0 variations in quantitative T-2 measurements using MRI. Magn. Reson. Med 2000a;43:589–93. [PubMed: 10748435]

Sled JG, Pike GB. Quantitative interpretation of magnetization transfer in spoiled gradient echo MRI sequences. J. Magn. Reson 2000b;145:24–36. [PubMed: 10873494]

Sogami M, Era S, Kinosada Y, Matsushima S, Kato K, Tomida M, Hirabayashi T. Basic studies on the equivalent cross-relaxation rate imaging (equivalent CRI)—phantom studies. NMR Biomed 2001;14:367–75. [PubMed: 11599035]

Tofts PS, Cercignani M, Tozer DJ, Ramani A, Barker GJ. Quantitative magnetization transfer mapping of bound protons in multiple sclerosis. Magn. Reson. Med 2005;53:492–3.erratum

Tozer D, Ramani A, Barker GJ, Davies GR, Miller DH, Tofts PS. Quantitative magnetization transfer mapping of bound protons in multiple sclerosis. Magn. Reson. Med 2003;50:83–91. [PubMed: 12815682]

Wolff SD, Balaban RS. Magnetization transfer contrast (MTC) and tissue water proton relaxation *in vivo*. Magn. Reson. Med 1989;10:135–44. [PubMed: 2547135]

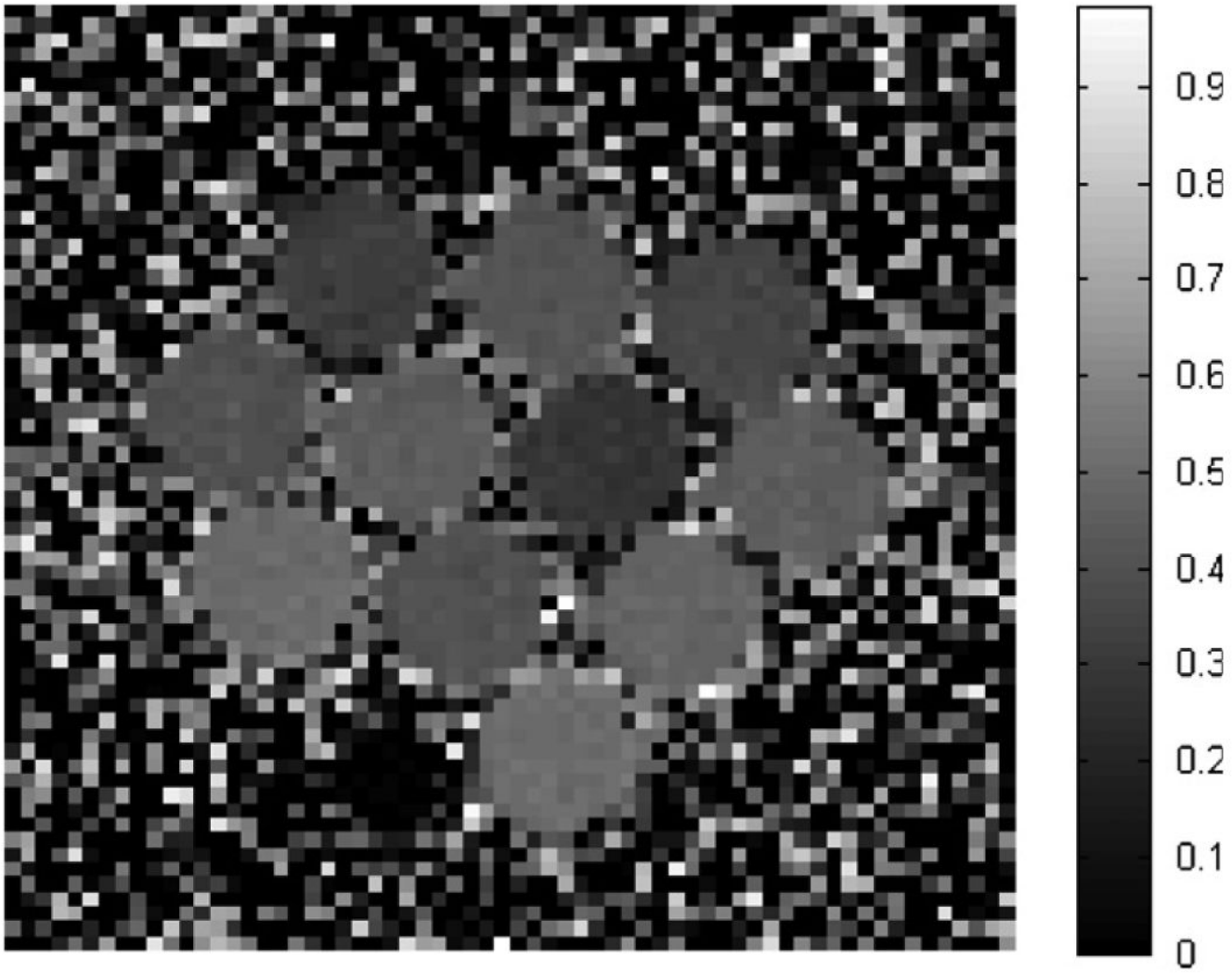

Figure 1.
Example MTP image for the MAGIC-2 dosimeter, acquired at 8.88 μT calculated from images acquired at 200 000 and 1375 Hz off-resonance. The dose values are, beginning at the top left and reading left to right, (row 1) 2, 10, 4 Gy; (row 2) 6, 12, 9, 14 Gy; (row 3) 18, 8, 16 Gy and (row 4) 20 Gy. The dark space to the left of the 20 Gy dosimeter is a small vial of water used for location reference purposes.

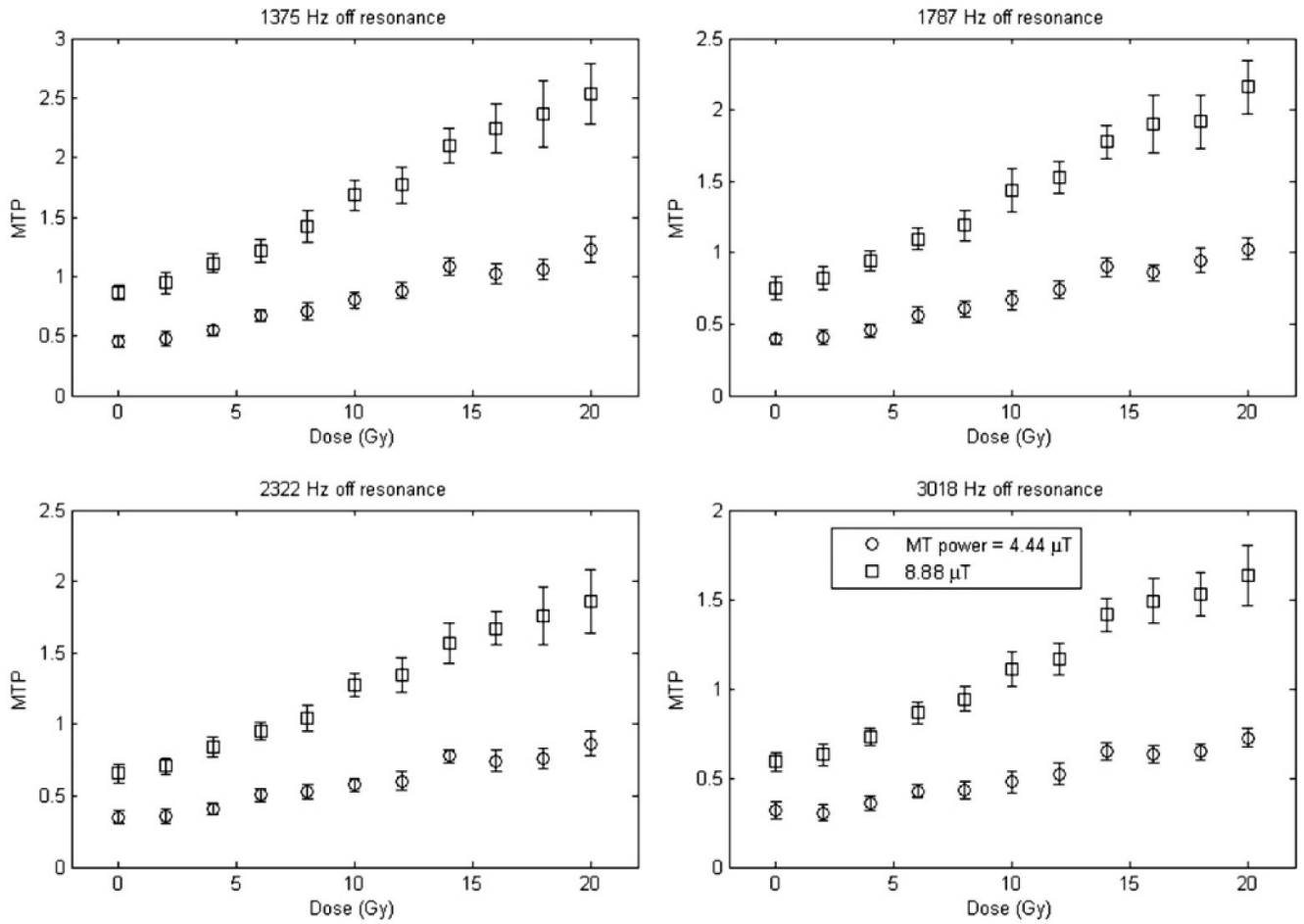

Figure 2.
MTP versus dose for the MAGIC dosimeter.

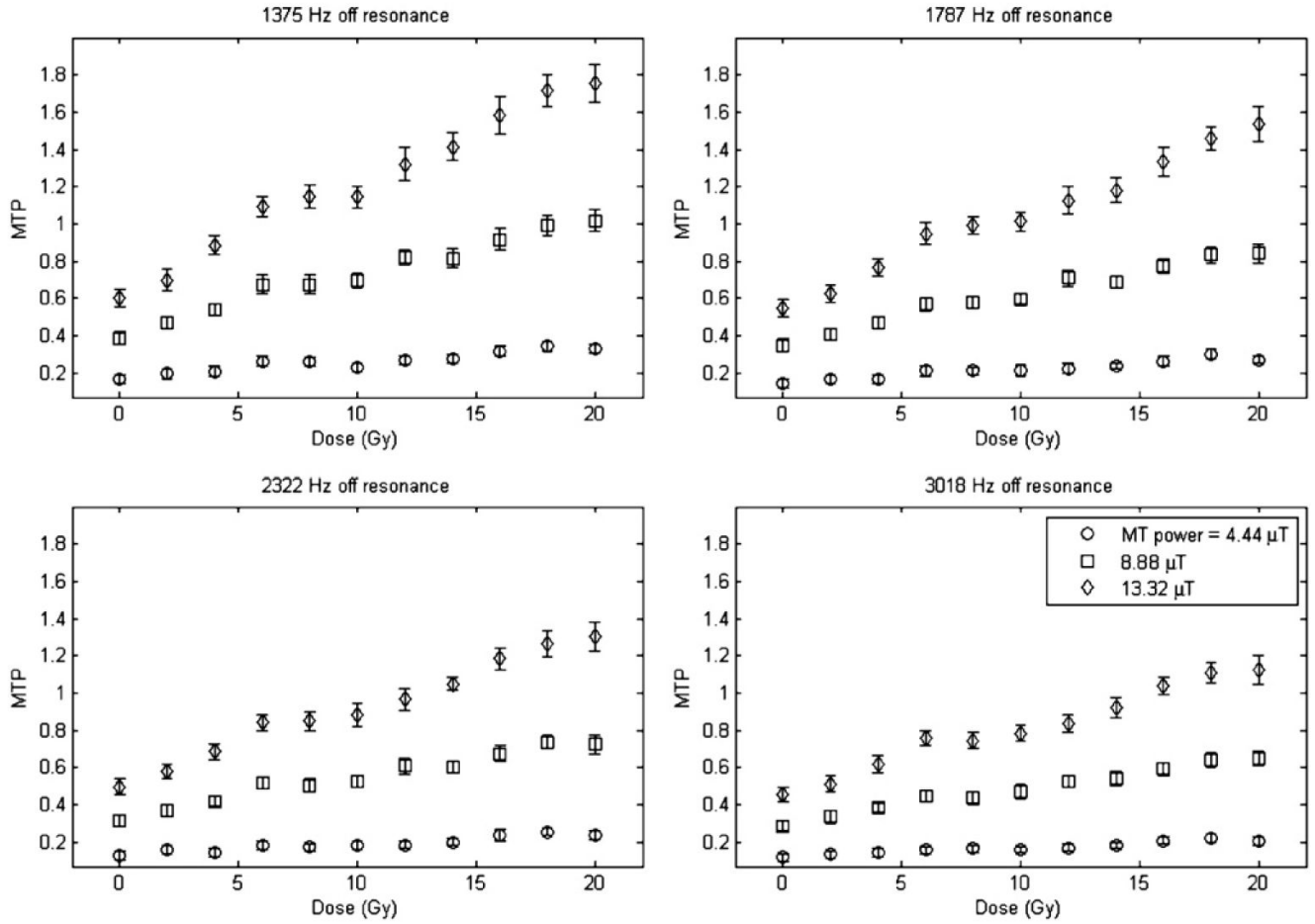

Figure 3.
MTP versus dose for the MAGIC-2 dosimeter.

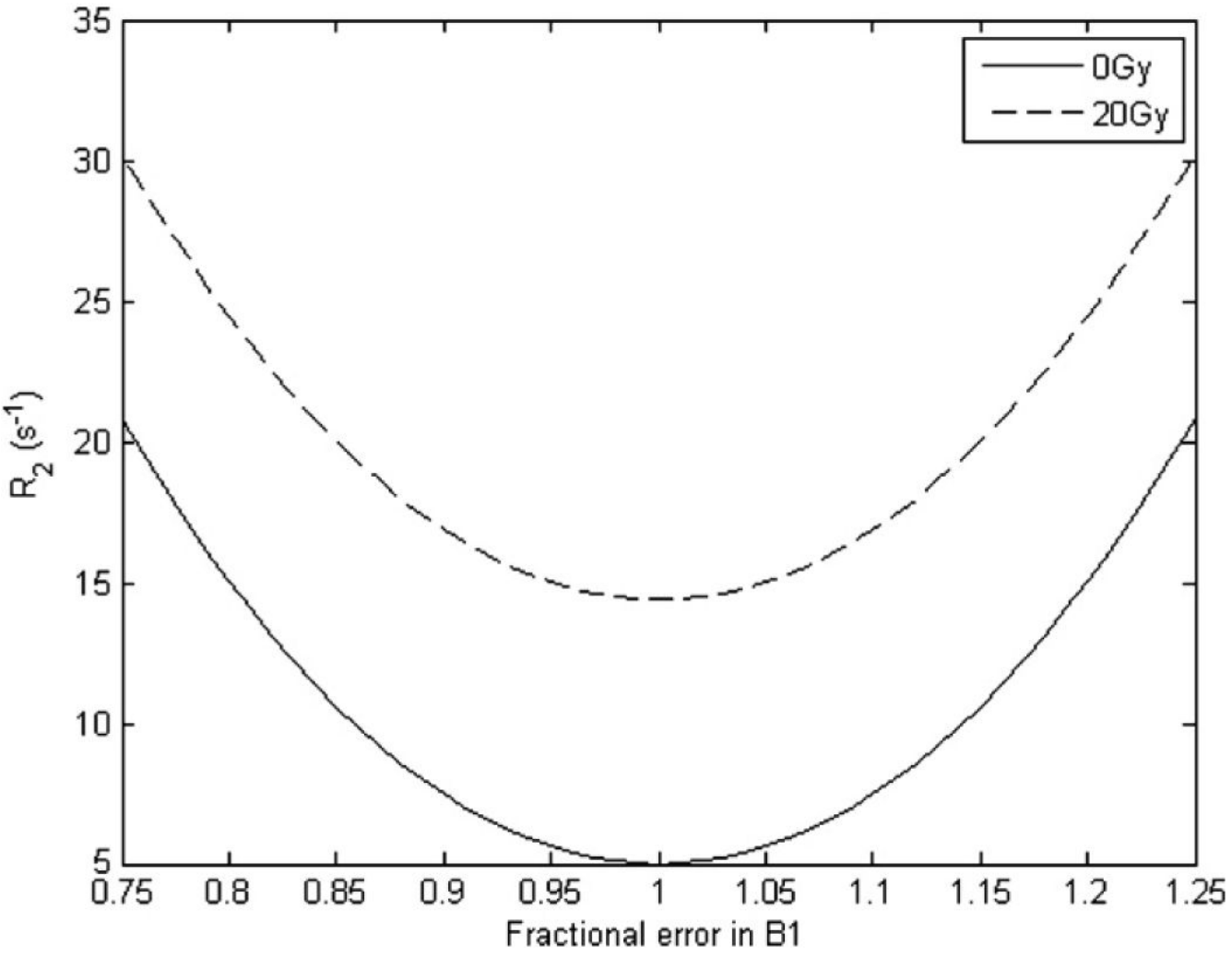

Figure 4.
Expected variation in R_2 for a given error in B_1 angle for the MAGIC dosimeter.

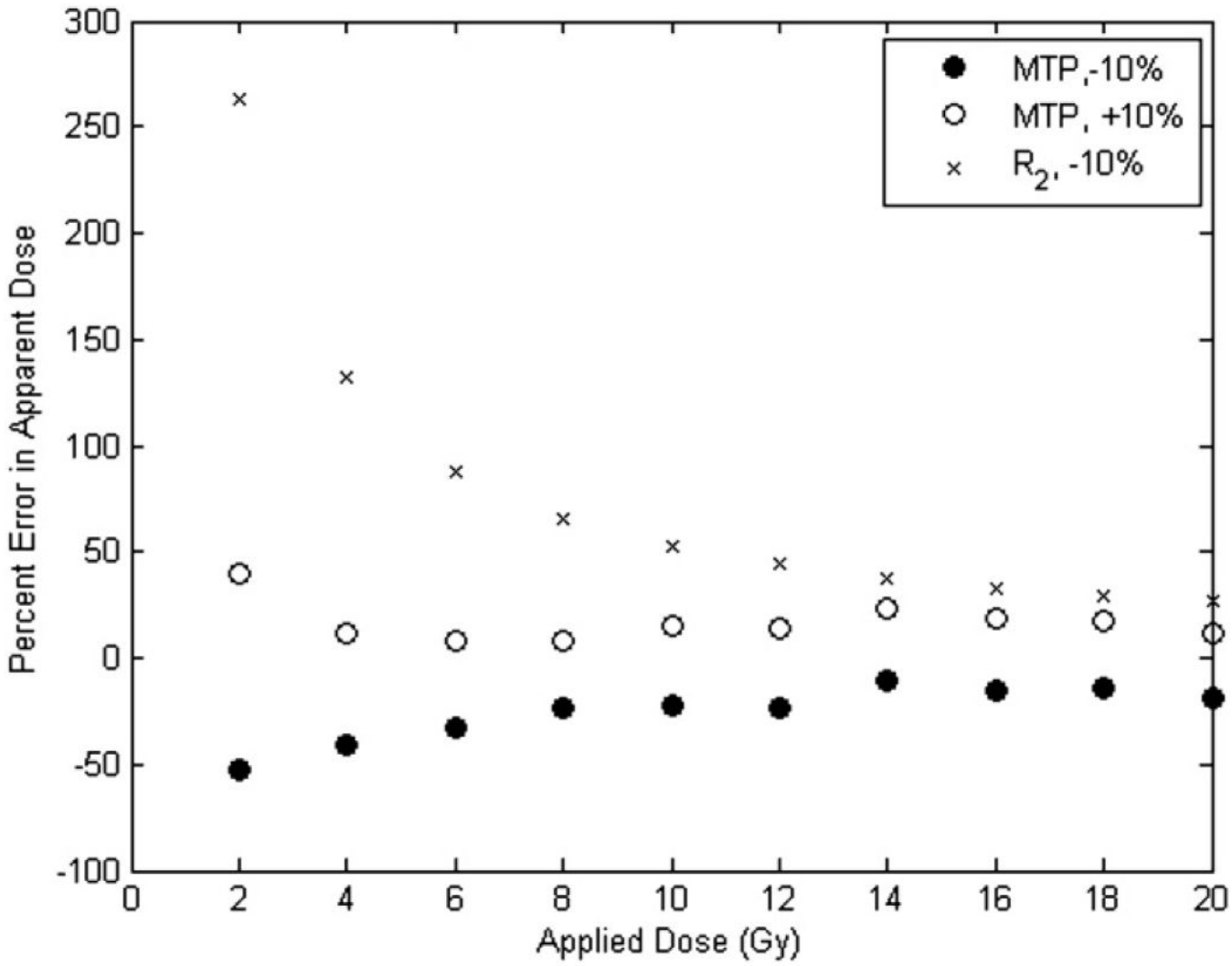

Figure 5.

Percent error in the apparent dose for MTP measurements at ±10% B_1 error and R_2 measurements at 10% error in the MAGIC gel dosimeter. The MTP data were acquired at MT power 7.92 (−10% error) and 9.68 (+10% error) μT and offset frequency 1375 Hz. The R_2 data were calculated by simulation using data from figure 4. Corresponding data for the MAGIC-2 dosimeter show an expected percent error in apparent dose for R_2 at 2 Gy to be approximately 217%, while the percent error for the MTP was an average of 96%. At 4 Gy, the percent error in R_2 was approximately 109%, while the percent error for the MTP was an average of 54%. With a few exceptions, the data followed this trend for all offset frequencies investigated (1375, 1787, 2322 and 3018 Hz off-resonance).

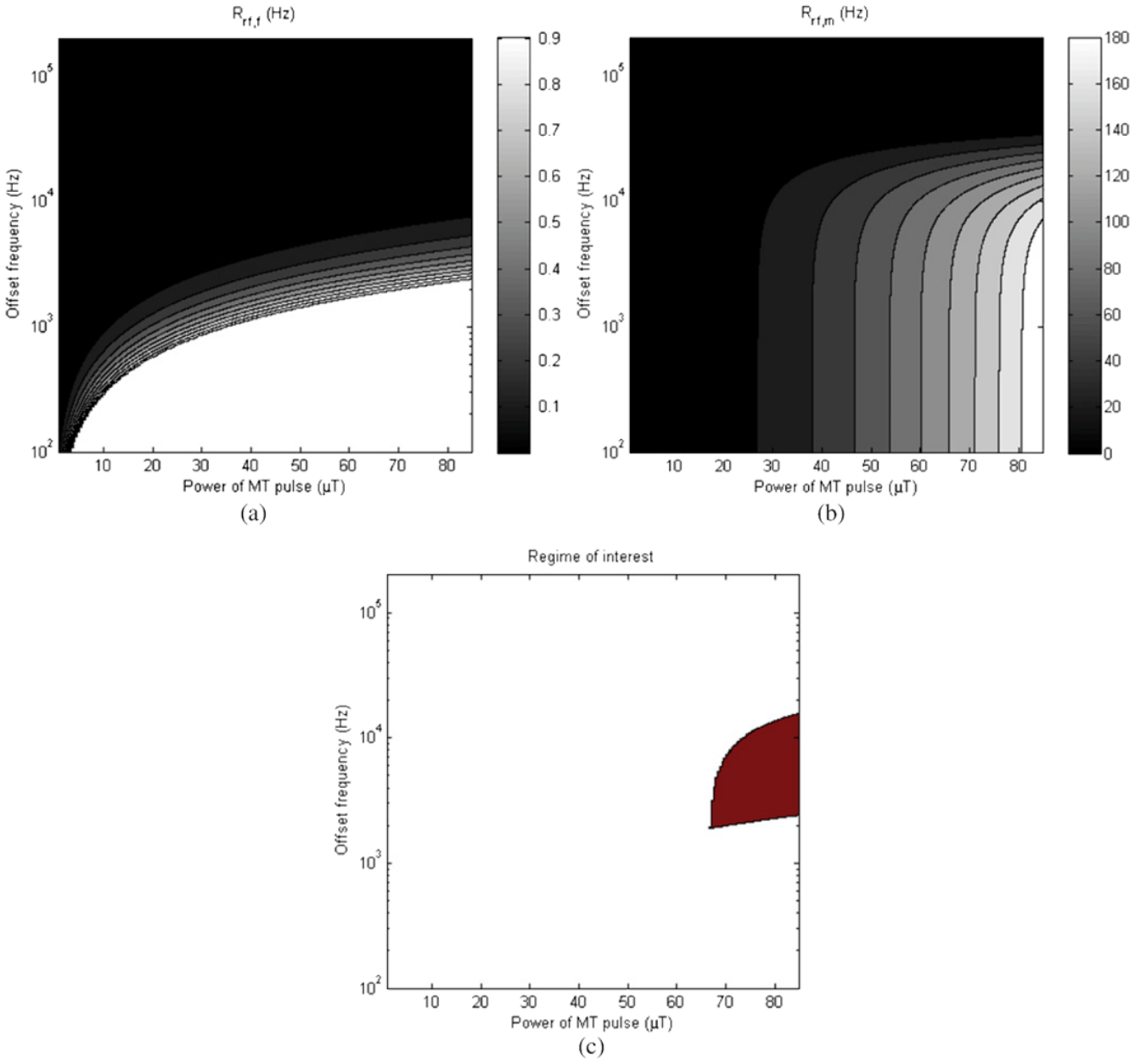

Figure 6.
(a) $R_{rf,f}$ for a 20 Gy MAGIC gel dosimeter, (b) $R_{rf,m}$ and (c) region for which the two criteria ($R_{rf,f}$ much less than all other rates, $R_{rf,m}$ much more than all other rates) overlap.

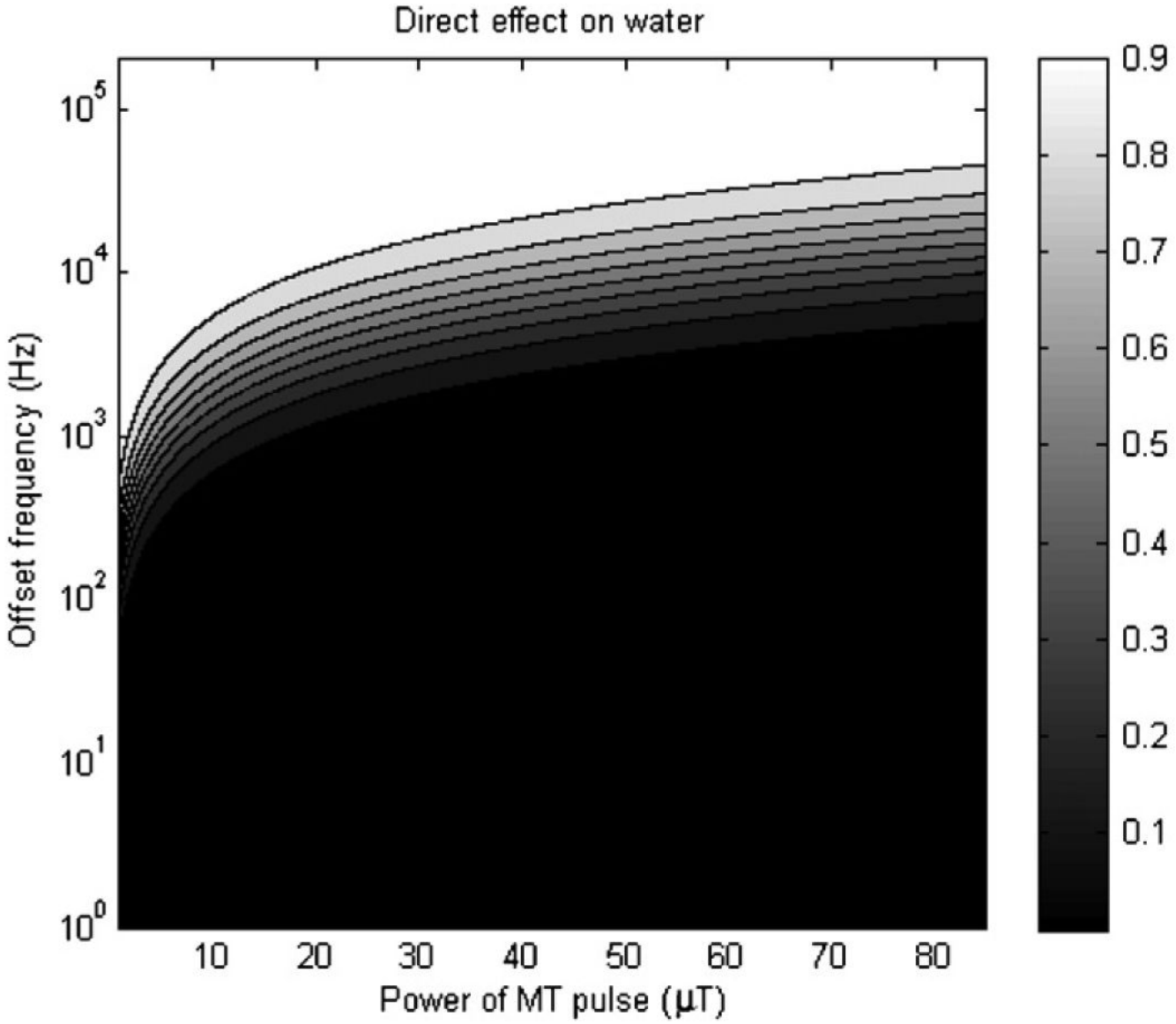

Figure 7.
Simulation of the direct effect on water for a range of offset frequencies and MT powers.

Table 1

R^2 for the measurement of the linearity of MTP versus dose, for the MAGIC gel dosimeter.

Offset frequency	MT power = 4.44 μT	MT power = 8.88 μT
1375	0.969	0.989
1787	0.979	0.988
2322	0.961	0.990
3018	0.962	0.985

Table 2

R^2 for the measurement of the linearity of MTP versus dose, for the MAGIC-2 gel dosimeter.

Offset frequency	MT power = 4.44 μT	MT power = 8.88 μT	MT power = 13.32 μT
1375	0.894	0.976	0.982
1787	0.925	0.975	0.983
2322	0.896	0.966	0.982
3018	0.923	0.981	0.976

Table 3

Measured slope of the MTP versus dose line for a variety of MT powers and offset frequencies for the MAGIC-2 dosimeter.

	Error in B_1 pulse angle				
Offset frequency	**−10%**	**−5%**	**No error**	**+5%**	**+10%**
MT power = 4.44 μT					
1375	0.0070	0.0071	0.0081	0.0089	0.0116
1787	0.0056	0.0054	0.0069	0.0070	0.0093
2322	0.0043	0.0044	0.0058	0.0055	0.0072
3018	0.0032	0.0034	0.0047	0.0042	0.0061
MT power = 8.88 μT					
1375	0.0254	0.0291	0.0308	0.0335	0.0361
1787	0.0205	0.0228	0.0247	0.0279	0.0299
2322	0.0170	0.0186	0.0209	0.0237	0.0248
3018	0.0140	0.0153	0.0178	0.0185	0.0207
MT power = 13.32 μT					
1375	0.0521	0.0537	0.0580	0.0621	0.0677
1787	0.0425	0.0461	0.0480	0.0520	0.0578
2322	0.0341	0.0382	0.0399	0.0443	0.0467
3018	0.0294	0.0314	0.0338	0.0377	0.0409

Table 4

Measured intercept of the MTP versus dose line for a variety of MT powers and offset frequencies for the MAGIC-2 dosimeter.

	Error in B_1 pulse angle				
Offset frequency	**−10%**	**−5%**	**No error**	**+5%**	**+10%**
MT power = 4.44 μT					
1375	0.1467	0.1639	0.1790	0.1944	0.1776
1787	0.1273	0.1448	0.1505	0.1704	0.1635
2322	0.1233	0.1270	0.1323	0.1549	0.1408
3018	0.1086	0.1130	0.1221	0.1427	0.1273
MT power = 8.88 μT					
1375	0.3656	0.3825	0.4207	0.4388	0.4621
1787	0.3252	0.3530	0.3730	0.3904	0.4173
2322	0.2875	0.3254	0.3367	0.3546	0.3825
3018	0.2668	0.2986	0.3051	0.3285	0.3428
MT power = 13.32 μT					
1375	0.5549	0.6145	0.6343	0.6519	0.6899
1787	0.5121	0.5400	0.5681	0.5757	0.6068
2322	0.4718	0.4948	0.5196	0.5256	0.5704
3018	0.4247	0.4572	0.4718	0.4783	0.5083

Table 5

Measured percent change in the slope-to-intercept ratio of the MTP versus dose line for a variety of MT powers and offset frequencies for the MAGIC dosimeter. For most powers and offset frequencies, the slope-to-intercept ratio does not vary more than 10% for even a 10% error in B_1 pulse angle.

	Error in B_1 pulse angle				
Offset frequency	**−10%**	**−5%**	**No error**	**+5%**	**+10%**
MT power = 4.44 μT					
1375	−0.61%	−1.73%	0.0941	−1.39%	10.05%
1787	−12.68%	−11.43%	0.0941	−0.92%	5.96%
2322	−3.80%	0.87%	0.0815	6.87%	18.92%
3018	−11.07%	−6.75%	0.0766	12.06%	13.41%
MT power = 8.88 μT					
1375	−6.17%	0.42%	0.1151	5.51%	3.11%
1787	6.16%	5.15%	0.1058	10.53%	14.42%
2322	−5.31%	4.14%	0.1087	0.45%	12.76%
3018	−3.03%	−4.00%	0.1051	8.16%	8.78%

Table 6

Measured percent change in the slope-to-intercept ratio of the MTP versus dose line for a variety of MT powers and offset frequencies for the MAGIC-2 dosimeter. With the exception of the values acquired at the lowest power, the slope-to-intercept ratio does not vary more than 10% for even a 10% error in B_1 pulse angle.

	Error in B_1 pulse angle				
Offset frequency	**−10%**	**−5%**	**No error**	**+5%**	**+10%**
MT power = 4.44 μT					
1375	5.93%	−4.48%	0.0452	1.38%	44.15%
1787	−3.49%	−19.47%	0.0459	−10.51%	23.44%
2322	−19.66%	−20.44%	0.0436	−18.69%	17.91%
3018	−24.73%	−22.81%	0.0386	−23.05%	24.66%
MT power = 8.88 μT					
1375	−5.16%	4.06%	0.0732	4.20%	6.86%
1787	−5.21%	−2.57%	0.0663	7.60%	7.87%
2322	−4.26%	−7.91%	0.0619	7.88%	4.58%
3018	−9.82%	−12.34%	0.0584	−3.33%	3.40%
MT power = 13.32 μT					
1375	2.64%	−4.54%	0.0915	4.04%	7.18%
1787	−1.66%	0.97%	0.0845	6.83%	12.74%
2322	−5.67%	0.57%	0.0767	10.00%	6.81%
3018	−3.25%	−3.92%	0.0715	10.06%	12.34%

Table 7

Expected change in the slope, intercept and slope–intercept ratio of R_2 versus dose for inclusion of B_1 angle error. Negative percent error in B_1 angle is not included as the result is symmetrical about zero percent error in B_1.

	Percent error in B_1 angle		
	0%	**5%**	**10%**
MAGIC			
Slope (s^{-1} Gy^{-1})	0.470	0.470	0.470
Intercept (s^{-1})	5.000	5.618	7.4778
Slope–intercept ratio	0.094	0.0834	0.063
Percent change in the slope–intercept ratio	—	−10.99%	−33.13%
MAGIC-2			
Slope (s^{-1} Gy^{-1})	0.570	0.570	0.570
Intercept (s^{-1})	6.290	6.908	8.768
Slope–intercept ratio	0.091	0.083	0.066
Percent change in the slope–intercept ratio	—	−8.94%	−28.26%